UDC 519.6 *http://dx.doi.org/10.30970/vam.2024.34.00000*

ON THE NON-LINEAR INTEGRAL EQUATION METHOD FOR THE INVERSE BOUNDARY RECONSTRUCTION PROBLEM

R. Chapko, S. Seniv

Ivan Franko National University of Lviv,
1, Universytetska str., 79000, Lviv, Ukraine,
e-mail: roman.chapko@lnu.edu.ua, sofiia.seniv.pmp@lnu.edu.ua

This paper is concerned with the reconstruction of an interior boundary curve in a planar double-connected domain from given Cauchy data of the harmonic function prescribed on the outer boundary. By employing single-layer potential representations, we reduce the problem to a system of non-linear boundary integral equations. Two iterative methods based on the Newton's linearization are proposed and implemented for numerical solving the system. The Fréchet derivatives of the corresponding integral operators are computed. Full discretization is achieved using quadrature and collocation methods. To resolve ill-posedness of the resulting linear system, we apply Phillips-Tikhonov regularization. An initial approximation for the interior boundary is found by the line method and a size estimation algorithm. Both methods are founded on finding the minimum of special functionals that include the given Cauchy data. Numerical examples confirm the stability, accuracy, and computational efficiency of the proposed approaches.

Key words: inverse problem, non-linear problem, boundary reconstruction, doubly-connected domain, single-layer potential, integral equation method, quadrature method, Fréchet derivative, Phillips-Tikhonov regularization.

1. Introduction

The mathematical formulation of inverse problems arising in nondestructive diagnostics of materials naturally leads to inverse boundary value problems for elliptic partial differential equations. In such problems, an unknown crack or inclusion must be reconstructed from boundary measurements, often available only on a subset of the outer boundary. Among the most efficient approaches to these inverse problems are those based on non-linear boundary integral equations, followed by the application of regularized iterative methods.

The idea of transforming an inverse boundary or inclusion problem into a non-linear integral equation system and solving it via iterative regularized schemes was systematically developed in a series of works, particularly for the Laplace and Navier equations.

Kress and Rundell in [9] introduced an iterative algorithm for non-linear integral equations focused on inverse source problems, establishing foundational convergence results. In [5] this approach was extended to handle inverse boundary value problems with inclusions and cracks. It uses the reciprocity gap functional with adapted boundary integral equations to reconstruct the unknown shape from Cauchy data. In [1] authors adressed boundary reconstruction in double-connected planar domains, showing the implementation of three different iterative approaches. The methods emphasize the use of Green's function for solving inverse boundary value problems, offering advantages over the reciprocity gap approach. The paper relates to disk-shaped domains where the Green's function can be explicitly constructed. In [2] it was applied non-linear integral

equations to reconstruct inclusions within elastic bodies, incorporating elasticity's vectorial nature to solve physically realistic inverse problems. In this paper our goal is to apply potential theory to derive a system of non-linear integral equations equivalent to an inverse boundary value problem for the Laplace equation.

The plan of the paper is as follows. In Section 2 we reduce the inverse boundary value problem (1) – (4) to three boundary integral equations using single-layer potential. Section 3 contains two iterative schemes for the numerical solution of the non-linear integral equations. The determination of the initial guess is discussed in Section 4. Section 5 contains the numerical example illustrating the feasibility of the non-linear integral equation method for approximate solution of the inverse boundary value problem.

Let $D_l \subset \mathbb{R}^2$ be bounded domains with boundaries Γ_l, $l = 1, 2$ such that $\bar{D}_1 \subsetneq D_2$. We denote the domain $D = D_2 \backslash \bar{D}_1$ with the boundary $\Gamma = \Gamma_1 \cup \Gamma_2$. Physically, Γ_1 represents the boundary of an unknown cavity, while Γ_2 corresponds to the accessible outer boundary.

For a given function $f_2 \in H^{1/2}(\Gamma_2)$ let the function $u \in H^1(D, \Delta)$ satisfies the Laplace equation

$$\Delta u = 0 \quad \text{in } D \tag{1}$$

and Dirichlet boundary value conditions

$$u = 0 \quad \text{on } \Gamma_1, \tag{2}$$

$$u = f_2 \quad \text{on } \Gamma_2. \tag{3}$$

The inverse boundary problem is to reconstruct the boundary $\Gamma_1 \in C^2$ from given the boundary $\Gamma_2 \in C^2$, Dirichlet data f_2 and the associated Neumann data

$$\frac{\partial u}{\partial \nu} = g_2 \quad \text{on } \Gamma_2, \tag{4}$$

where $\nu = (\nu_1, \nu_2)$ denotes the outward unit normal vector and $g_2 \in H^{-1/2}(\Gamma_2)$ is a given function.

Note that we a priori know that the domain D_2 contains exactly one cavity with boundary Γ_1, and our goal is to reconstruct the shape of this cavity, i.e., the curve Γ_1.

Next result follows from the unique continuation property of harmonic functions (see [4]).

Theorem 1. *Let D and $\tilde{D}$ be two bounded domains with a common outer boundary Γ_2 and respective inner boundaries Γ_1 and $\tilde{\Gamma}_1$. Denote by u and $\tilde{u}$ the solutions to the Dirichlet problem in D and $\tilde{D}$, respectively. Suppose that $f_2 \not\equiv 0$ and*

$$\frac{\partial u}{\partial \nu} = \frac{\partial \tilde{u}}{\partial \nu}$$

on an open subset of Γ_2. Then it follows that $\Gamma_1 = \tilde{\Gamma}_1$.

Therefore, Theorem 1 ensures the uniqueness of the boundary Γ_1 corresponding to the prescribed Cauchy data (f_2, g_2) on Γ_2. The inverse boundary problem (1)–(4) is, however, ill-posed due to the lack of stability: small perturbations (e.g., noise) in the data on Γ_2 may lead to arbitrarily large errors in the reconstruction of Γ_1. Moreover, the problem is non-linear, since the Cauchy data on Γ_2 depend non-linearly on the boundary Γ_1.

2. Potential-based integral equation approach

To transform the problem into an integral equation formulation, we express the solution using layer potentials. Firstly, let us introduce the fundamental solution to Laplace equation

$$\Phi(x,y)=\frac{1}{2\pi}\ln\frac{1}{|x-y|},\ x\neq y.$$

We represent the function u from the inverse boundary problem (1)-(4) as the combination of single-layer potentials

$$u(x)=\sum_{l=1}^{2}\int_{\Gamma_l}\mu_l(y)\Phi(x,y)ds(y),\ x\in D,$$

where $\mu_l\in H^{-1/2}(\Gamma_l),\ l=1,2$ are unknown densities.

Taking into consideration the continuity property of the single-layer potential and so called jump in its normal derivative across the boundary, we obtain

$$u(x)=(S_{1l}\mu_1)(x)+(S_{2l}\mu_2)(x),\ x\in\Gamma_l,\ l=1,2 \tag{5}$$

and

$$\frac{\partial u}{\partial\nu}(x)=\frac{1}{2}\mu_2(x)+(D_1\mu_1)(x)+(D_2\mu_2)(x),\ x\in\Gamma_2, \tag{6}$$

where the boundary integral operators $S_{kl}:H^{-1/2}(\Gamma_k)\to H^{1/2}(\Gamma_l)$ and $D_l:H^{-1/2}(\Gamma_l)\to H^{-1/2}(\Gamma_l)$ are defined

$$(S_{kl}\mu)(x)=\int_{\Gamma_k}\mu(y)\Phi(x,y)ds(y),\ x\in\Gamma_l,$$

$$(D_l\mu)(x)=\int_{\Gamma_l}\mu(y)\frac{\partial\Phi(x,y)}{\partial\nu(x)}ds(y),\ x\in\Gamma_2.$$

Satysfying the boundary conditions (2) – (3), we receive from (5) a non-linear system of boundary integral equations

$$\begin{cases} S_{11}\mu_1+S_{21}\mu_2=0 & \text{on } \Gamma_1,\\ S_{12}\mu_1+S_{22}\mu_2=f_2 & \text{on } \Gamma_2. \end{cases} \tag{7}$$

The condition (4) and representation (6) leads to the integral equation

$$\frac{1}{2}\mu_2+D_1\mu_1+D_2\mu_2=g_2 \qquad \text{on } \Gamma_2. \tag{8}$$

The equations (7) are called the "field" equations and equation (8) is called "data" equation.

Thus, the formulated inverse boundary problem (1)-(4) is redused to the system of non-linear integral equations (7)-(8). We note here that for given boundaries $\Gamma_l,\ l=1,2$ the system of integral equations (7) is well-posed problem in corresponding spaces [7].

3. Two iterative algorithms for a non-linear system of integral equations

In order to solve the system we transform the line integrals over the curve into definite integrals over a fixed interval by parametrizing the boundary. We assume that the boundary Γ_2 is given in parametric form

$$\Gamma_2 = \{x_2(t) = (x_{21}(t), x_{22}(t)),\ |x_2'(t)| > 0,\ t \in [0, 2\pi]\},$$

where $x_{21}, x_{22} \in C^2[0, 2\pi]$.

For computational simplicity, we consider the reconstruction of Γ_1 in the class of starlike curves, which have the following parametric form

$$\Gamma_1 = \{x_1(t) = r(t)c(t),\ |x_1'(t)| > 0,\ t \in [0, 2\pi]\},$$

where $c(t) = (\cos t, \sin t)$ and $r : \mathbb{R} \to (0, \infty)$ is a 2π-periodic twice continuously differentiable function representing the radial distance from the origin.

This allows the operator S_{kl} to be represented in a parametric form

$$(\tilde{S}_{kl}\varphi)(t) = \frac{1}{2\pi}\int_0^{2\pi} \varphi(\tau)K_{kl}(t,\tau)d\tau,$$

where $K_{kl}(t,\tau) = 2\pi\Phi(x_k(t), x_l(\tau)),\ k,l = 1,2$.

Due to the logarithmic singularity in the kernels $K_{ll},\ l = 1,2$, it is convenient to use additive decomposition. Accordingly, we write them as

$$K_{ll}(t,\tau) = -\frac{1}{2}\ln\left(\frac{4}{e}\sin^2\frac{t-\tau}{2}\right) + \tilde{K}_{ll}(t,\tau),$$

where

$$\tilde{K}_{ll}(t,\tau) = \begin{cases} \dfrac{1}{2}\ln\dfrac{\frac{4}{e}\sin^2\frac{t-\tau}{2}}{|x_l(t) - x_l(\tau)|^2},\ t \neq \tau, \\ \dfrac{1}{2}\ln\dfrac{1}{e|x_l'(t)|^2},\ t = \tau. \end{cases}$$

The parametrization of the operators $D_l,\ l = 1,2$ leads to the following representation

$$(\tilde{D}_l\varphi)(t) = \frac{1}{2\pi}\int_0^{2\pi} \varphi(\tau)L_{2l}(t,\tau)d\tau,\ l = 1,2,$$

where

$$L_{2l}(t,\tau) = \frac{\nu(x_2(t))\cdot(x_l(\tau) - x_2(t))}{|x_l(\tau) - x_2(t)|^2}, \quad l = 1,2$$

with

$$L_{22}(t,t) = \frac{x_2''(t)\cdot\nu(x_2(t))}{2|x_2'(t)|^2}.$$

Thus, the system (7) – (8) can be rewritten in the parametric form

$$\begin{cases} \tilde{S}_{11}\varphi_1 + \tilde{S}_{12}\varphi_2 = 0 & \text{on } [0,2\pi], \\ \tilde{S}_{21}\varphi_1 + \tilde{S}_{22}\varphi_2 = \tilde{f}_2 & \text{on } [0,2\pi], \end{cases} \tag{9}$$

$$\tilde{D}_1\varphi_1 + \hat{D}_2\varphi_2 = \tilde{g}_2 \qquad \text{on } [0, 2\pi], \tag{10}$$

where $\tilde{f}_2(t) = f_2(x_2(t))$, $\tilde{g}_2(t) = g_2(x_2(t))$, $\varphi_k(\tau) = \mu_k(x_k(\tau))|x_k'(\tau)|$ and

$$(\hat{D}_2\varphi)(t) = \frac{1}{2}\frac{\varphi(t)}{|x_2'(t)|} + (\tilde{D}_2\varphi)(t).$$

The determination of the boundary Γ_1 is a non-linear problem. One of the classical approaches to its solution is the Newton iterative method. Therefore, the algorithms presented below are based on the application of this method and involve the linearization of the integral equation. In this way, at each iteration step, the solution is refined, leading to a more accurate reconstruction of the internal boundary.

Algorithm A.

1. Set an initial value for r.
2. Solve the well-posed in corresponding Sobolev spaces system of parametrized integral equations (9) with respect to φ_1 and φ_2.
3. For the given r, φ_1 та φ_2 solve the ill-posed system of linearized integral equations

$$\begin{cases} \tilde{S}_{11}\phi_1 + \tilde{S}_{12}\phi_2 + \tilde{S}_{11}'[r,\varphi_1]q + \tilde{S}_{12}'[r,\varphi_2]q = -\tilde{S}_{11}\varphi_1 - \tilde{S}_{12}\varphi_2, \\ \tilde{S}_{21}\phi_1 + \tilde{S}_{22}\phi_2 + \tilde{S}_{21}'[r,\varphi_1]q = \tilde{f}_2 - \tilde{S}_{21}\varphi_1 - \tilde{S}_{22}\varphi_2, \\ \tilde{D}_1\phi_1 + \hat{D}_2\phi_2 + \tilde{D}_1'[r,\varphi_1]q = \tilde{g}_2 - \tilde{D}_1\varphi_1 - \hat{D}_2\varphi_2 \end{cases} \tag{11}$$

   with respect to q, ϕ_1 and ϕ_2. Here $\tilde{S}_{kl}'$ and $\tilde{D}_1'$ denote the Fréchet derivatives of the corresponding integral operators with respect to the radial function r. A more detailed description of these operators is provided in the next section. The system (11) is obtained from (9)–(10) by linearization with respect to all unknown functions. In this derivation, we take into account that the integral operators are linear with respect to the densities.
4. Update the radial function $r = r + \zeta q$ and densities $\varphi_1 = \varphi_1 + \phi_1, \varphi_2 = \varphi_2 + \phi_2$. Here $\zeta \in (0, 1)$ is the relaxation parameter.
5. Repeat steps 3 — 4 until the stopping criterion is satisfied

$$\frac{||q||_{L^2[0,2\pi]}}{||r||_{L^2[0,2\pi]}} < \epsilon,$$

   where ϵ is the given tolerance.

We note here that analogously to [1] it can be shown that if the functions q, ϕ_1 and ϕ_2 satisfy the homogeneous system corresponded to (11), then the only possible solution is the trivial one.

Algorithm B.

1. Set an initial value for r.
2. Solve the well-posed system of parameterized integral equations (9) with respect to φ_1 and φ_2.
3. For the given r, φ_1 та φ_2 solve the linearized integral equation

$$\tilde{D}_1'[r,\varphi_1]q = \tilde{g}_2 - \tilde{D}_1\varphi_1 - \hat{D}_2\varphi_2 \tag{12}$$

   with respect to q.

4. Update the radial function $r = r + \xi q$, where $\xi \in (0,1)$ is the relaxation parameter.
5. Repeat steps 2 — 4 until the stopping criterion is satisfied

$$\frac{||q||_{L^2[0,2\pi]}}{||r||_{L^2[0,2\pi]}} < \epsilon.$$

Similar to Algorithm A, linearized equation (12) has a unique solution.

These two iterative schemes differ in complexity and convergence behavior. Method A typically converges faster and provides more accurate updates per step, as it fully accounts for the non-linear coupling between variables. However, it comes with increased computational cost and requires solving a larger system. In contrast, Method B employs a simpler structure by updating the boundary shape based solely on a single linearized equation related to the shape derivative. It usually converges more slowly.

The stopping criterion employed in both methods is designed to control the growth of the iterative process. It is expressed in the L^2 norm, since the data discrepancy is naturally measured in this space.

3.1. Implementation of algorithm A

Step 1. To numerically solve the system of integral equations (9), we employ a quadrature method, which consists in approximating the integral operators using appropriate quadrature rules. Specifically, for integrals with smooth and continuous kernels, we apply the trapezoidal rule, which is particularly effective in the context of periodic parametrizations due to its spectral convergence properties. For integrals involving logarithmic singularities, we use trigonometric quadrature formulas that accurately handle such singular behavior. Thus, the following quadrature rules [7], [8] are used

$$\frac{1}{2\pi}\int_0^{2\pi} g(\tau)d\tau \approx \frac{1}{2n}\sum_{j=0}^{2n-1} g(t_j), \tag{13}$$

$$\frac{1}{2\pi}\int_0^{2\pi} g(\tau)\ln\left(\frac{4}{e}\sin^2\frac{t-\tau}{2}\right)d\tau \approx \sum_{j=0}^{2n-1} g(t_j)R_j(t), \tag{14}$$

where $R_j(t) = -\frac{1}{n}\left\{\sum_{m=1}^{n-1}\frac{1}{m}\cos m(t-t_j) + \frac{1}{2n}\cos n(t-t_j)\right\} - \frac{1}{2n}$.

The quadrature nodes are chosen to be equidistant on the interval $[0,2\pi]$, defined as $t_j = \frac{j\pi}{n}$, $j = 0,\dots,2n-1$, $n \in \mathbb{N}$. By collocating the resulting discrete equations at the quadrature nodes, we obtain a linear system

$$\begin{cases} \sum\limits_{j=0}^{2n-1}\left\{\varphi_{1,n}(t_j)\left[-\frac{1}{2}R_j(t_k) + \frac{1}{2n}\tilde{K}_{11}(t_k,t_j)\right] + \varphi_{2,n}(t_j)\frac{1}{2n}K_{12}(t_k,t_j)\right\} = 0, \\ \sum\limits_{j=0}^{2n-1}\left\{\varphi_{1,n}(t_j)\frac{1}{2n}K_{21}(t_k,t_j) + \varphi_{2,n}(t_j)\left[-\frac{1}{2}R_j(t_k) + \frac{1}{2n}\tilde{K}_{22}(t_k,t_j)\right]\right\} = \tilde{f}_2(t_k), \end{cases}$$

where $\varphi_{l,n}(t_k) \approx \varphi_l(t_k)$, $l = 1,2$, $k = 0,\dots 2n-1$.

Step 2. According to the algorithm, we obtain a system of linearized equations that requires the computation of Fréchet derivatives. These derivatives can be explicitly

calculated by differentiating the kernels of the integral operators with respect to the radial function

$$(\tilde{S}'_{11}[r,\varphi_1]q)(t) = \frac{1}{2\pi}\int_0^{2\pi}\left[q(\tau)N_{11}^{(1)}(t,\tau) + q(t)N_{11}^{(2)}(t,\tau)\right]\varphi_1(\tau)d\tau,$$

$$(\tilde{S}'_{12}[r,\varphi_2]q)(t) = \frac{1}{2\pi}\int_0^{2\pi} q(t)N_{12}(t,\tau)\varphi_2(\tau)d\tau,$$

$$(\tilde{S}'_{21}[r,\varphi_1]q)(t) = \frac{1}{2\pi}\int_0^{2\pi} q(\tau)N_{21}(t,\tau)\varphi_1(\tau)d\tau,$$

$$(\tilde{D}'_{1}[r,\varphi_1]q)(t) = \frac{1}{2\pi}\int_0^{2\pi} q(\tau)N_{r}(t,\tau)\varphi_1(\tau)d\tau. \tag{15}$$

The kernels of the Fréchet derivatives are computed as follows

$$N_{11}^{(1)}(t,\tau) = c(\tau)\cdot\nabla_{x_1(\tau)}\tilde{K}_{11}(t,\tau) = c(\tau)\cdot\left(\frac{x_{11}(t)-x_{11}(\tau)}{|x_1(t)-x_1(\tau)|^2}, \frac{x_{12}(t)-x_{12}(\tau)}{|x_1(t)-x_1(\tau)|^2}\right),\ t\neq\tau$$

$$N_{12}(t,\tau) = c(t)\cdot\nabla_{x_1(t)}K_{12}(t,\tau) = c(t)\cdot\left(-\frac{x_{11}(t)-x_{21}(\tau)}{|x_1(t)-x_2(\tau)|^2}, -\frac{x_{12}(t)-x_{22}(\tau)}{|x_1(t)-x_2(\tau)|^2}\right),$$

$$N_r(t,\tau) = c(\tau)\cdot\nabla_{x_1(\tau)}L_{21}(t,\tau) = c(\tau)\cdot(v_1(t,\tau), v_2(t,\tau)),$$

where $v_k(t,\tau) = \dfrac{\nu_k(x_2(t)) - 2L_{21}(t,\tau)(x_{1k}(\tau)-x_{2k}(t))}{|x_1(\tau)-x_2(t)|^2},\ k=1,2.$

Obviously, $N_{21}(t,\tau) = N_{12}(\tau,t)$ and $N_{11}^{(2)}(t,\tau) = N_{11}^{(1)}(\tau,t)$. Also, taking the limit, the kernel

$$N_{11}(t,\tau) = \lim_{\tau\to t}\left[q(\tau)N_{11}^{(1)}(t,\tau) + q(t)N_{11}^{(2)}(t,\tau)\right] = -\frac{r(t)q(t)+r'(t)q'(t)}{r(t)^2+(r'(t))^2}.$$

The unknown correction q is determined using the collocation method, selecting basis functions from the space of trigonometric polynomials

$$q_m(t) = \sum_{i=0}^{2m} q_{mi}\ l_i(t),\ m\in\mathbb{N},$$

where $m<n$ and

$$l_i(t) = \begin{cases} \cos(it), & i=0,\cdots,m,\\ \sin((i-m)t), & i=m+1,\cdots,2m.\end{cases}$$

For the discretization of the system of integral equations (11), we employ the quadrature method. Specifically, we approximate the integrals using the trapezoidal rule (13). This leads to a system of linear equations

$$\begin{cases} \sum\limits_{j=0}^{2n-1}\phi_{nj}^{(1)}A_{ij}^{(11)} + \sum\limits_{j=0}^{2n-1}\phi_{nj}^{(2)}A_{ij}^{(12)} + \sum\limits_{j=0}^{2m} q_{mj}A_{ij}^{(13)} = B_i^{(1)},\\ \sum\limits_{j=0}^{2n-1}\phi_{nj}^{(1)}A_{ij}^{(21)} + \sum\limits_{j=0}^{2n-1}\phi_{nj}^{(2)}A_{ij}^{(22)} + \sum\limits_{j=0}^{2m} q_{mj}A_{ij}^{(23)} = B_i^{(2)},\\ \sum\limits_{j=0}^{2n-1}\phi_{nj}^{(1)}A_{ij}^{(31)} + \sum\limits_{j=0}^{2n-1}\phi_{nj}^{(2)}A_{ij}^{(32)} + \sum\limits_{j=0}^{2m} q_{mj}A_{ij}^{(33)} = B_i^{(3)},\end{cases}$$

where $\phi_{ni}^{(s)} = \phi_s(t_i),\ s = 1, 2,\ i = 0, \ldots, 2n-1$. The elements of the matrix are computed using the following formulas

$$A_{ij}^{(11)} = -\frac{1}{2}R_j(t_i) + \frac{1}{2n}\tilde{K}_{11}(t_i, t_j), \quad A_{ij}^{(12)} = \frac{1}{2n}K_{12}(t_i, t_j),$$

$$A_{ij}^{(21)} = \frac{1}{2n}K_{21}(t_i, t_j), \quad A_{ij}^{(22)} = -\frac{1}{2}R_j(t_i) + \frac{1}{2n}\tilde{K}_{22}(t_i, t_j),$$

$$A_{ij}^{(31)} = \frac{1}{2n}L_{21}(t_i, t_j), \qquad A_{ij}^{(32)} = \frac{1}{2|x_2'(t_i)|} + \frac{1}{2n}L_{22}(t_i, t_j),$$

$$A_{ij}^{13} = l_j(t_i)N_{12}(t_i, t_k)\varphi_{2,n}(t_k) + \frac{1}{2n}\begin{cases} \sum\limits_{k=0}^{2n-1} \varphi_{1,n}(t_k)\left[l_j(t_k)N_{11}^{(1)}(t_i, t_k) + \right. \\ \qquad\qquad \left. + l_j(t_i)N_{11}^{(2)}(t_i, t_k)\right],\ t_i \neq t_k, \\ \sum\limits_{k=0}^{2n-1} \varphi_{1,n}(t_k)N_{11}(t_i, t_k),\ t_i = t_k, \end{cases}$$

$$A_{ij}^{(23)} = \frac{1}{2n}\sum_{k=0}^{2n-1} l_j(t_k)N_{21}(t_i, t_k)\varphi_{1,n}(t_k), \qquad A_{ij}^{(33)} = \frac{1}{2n}\sum_{k=0}^{2n-1} l_j(t_k)N_r(t_i, t_k)\varphi_{1,n}(t_k),$$

$$B_i^{(1)} = -\sum_{k=0}^{2n-1}\left\{\varphi_{1,n}(t_k)\left[-\frac{1}{2}R_k(t_i) + \frac{1}{2n}\tilde{K}_{11}(t_i, t_k)\right] + \varphi_{2,n}(t_k)\frac{1}{2n}K_{12}(t_i, t_k)\right\},$$

$$B_i^{(2)} = \tilde{f}_2(t_i) - \sum_{k=0}^{2n-1}\left\{\varphi_{1,n}(t_k)\frac{1}{2n}K_{21}(t_i, t_k) + \varphi_{2,n}(t_k)\left[-\frac{1}{2}R_k(t_i) + \frac{1}{2n}\tilde{K}_{22}(t_i, t_k)\right]\right\},$$

$$B_i^{(3)} = \tilde{g}_2(t_i) - \frac{\varphi_{2,n}(t_i)}{2|x_2'(t_i)|} - \frac{1}{2n}\sum_{k=0}^{2n-1}\left\{L_{21}(t_i, t_k)\varphi_{1,n}(t_k) + L_{22}(t_i, t_k)\varphi_{2,n}(t_k)\right\}.$$

As it was mentioned before the inverse problems are ill-posed. Therefore, to stabilize the solution, regularization methods are employed, for example, Phillips–Tikhonov regularization and the method of least squares

$$\begin{cases} \alpha\phi_{ni}^{(1)} + \sum\limits_{j=0}^{2n-1}\phi_{nj}^{(1)}a_{ij}^{(11)} + \sum\limits_{j=0}^{2n-1}\phi_{nj}^{(2)}a_{ij}^{(12)} + \sum\limits_{j=0}^{2m} q_{mj}a_{ij}^{(13)} = b_i^{(1)},\ i = 0, \ldots, 2n-1, \\ \beta\phi_{ni}^{(2)} + \sum\limits_{j=0}^{2n-1}\phi_{nj}^{(1)}a_{ij}^{(21)} + \sum\limits_{j=0}^{2n-1}\phi_{nj}^{(2)}a_{ij}^{(22)} + \sum\limits_{j=0}^{2m} q_{mj}a_{ij}^{(23)} = b_i^{(2)},\ i = 0, \ldots, 2n-1, \\ \gamma q_{mi} + \sum\limits_{j=0}^{2n-1}\phi_{nj}^{(1)}a_{ij}^{(31)} + \sum\limits_{j=0}^{2n-1}\phi_{nj}^{(2)}a_{ij}^{(32)} + \sum\limits_{j=0}^{2m} q_{mj}a_{ij}^{(33)} = b_i^{(3)},\ i = 0, \ldots, 2m, \end{cases}$$

where $\alpha > 0, \beta > 0, \gamma > 0$ are regularization parameters and

$$a_{ij}^{(lp)} = \sum_{k=0}^{2n-1} A_{ki}^{(l1)}A_{kj}^{(p1)} + \sum_{k=0}^{2n-1} A_{ki}^{(l2)}A_{kj}^{(p2)} + \sum_{k=0}^{2m} A_{ki}^{(l3)}A_{kj}^{(p3)},$$

$$b_i^{(l)} = \sum_{k=0}^{2n-1} A_{ki}^{(l1)}B_k^{(1)} + \sum_{k=0}^{2n-1} A_{ki}^{(l2)}B_k^{(2)} + \sum_{k=0}^{2m} A_{ki}^{(l3)}B_k^{(3)}.$$

3.2. Implementation of algorithm B

Step 1. It is analogous to the Step 1 from the Algorithm A. Apart from Algorithm A the system of equations is solved iteratively at each step.

Step 2. The implementation of this step closely follows the approach established in the Algorithm A. Specifically, the computation of the Fréchet derivative, which is essential for the linearization step, is already computed (15) and can be reuse here. Similarly, the correction q is represented in the same space of trigonometric polynomials. The discretization of the integral equations using the trapezoidal rule remains unchanged, enabling the use of matrices $A_{ij}^{(33)}$ and vector $B_i^{(3)}$ previously defined.

Unlike the Algorithm A, which requires solving a coupled system involving the unknowns $\phi_1,\ \phi_2$ and q, this algorithm reduces the problem to solving a system that involves only the correction q. This reduction is achieved by forming a regularized system of linear equations of the form

$$\alpha q_{mi} + \sum_{j=0}^{2m} q_{mj} a_{ij} = b_i,\ i = 0, \cdots, 2m,$$

where the elements of the matrix and right-hand side vector are given by

$$a_{ij} = \sum_{k=0}^{2n-1} A_{ki}^{(33)} A_{kj}^{(33)}, \quad b_i = \sum_{k=0}^{2n-1} A_{ki}^{(33)} B_k^{(3)}.$$

Here, $\alpha > 0$ is the regularization parameter used to stabilize the ill-posed inverse problem, employing the Phillips–Tikhonov regularization technique.

4. Determination of the initial guess

To ensure the effective application of the previously discussed iterative methods, it is essential to obtain a suitable initial approximation of the unknown inclusion. In this section, we discuss two complementary algorithms aimed at identifying the approximate location and estimating the size of the inclusion. A well-chosen starting point is not only crucial for ensuring global convergence, but also for accelerating the overall computational process.

4.1. The line location search method

This method is based on an explicit analytical expression for determining the location of the inclusion (see [6]). This makes the algorithm straightforward to implement, as the result can be obtained by simply constructing two or more lines. Moreover, this approach offers excellent computational efficiency.

1. Define the functional

$$H(x, f, g) = \int_{\Gamma_2} \left[\frac{\partial \Phi(x, y)}{\partial \nu(y)} f(y) - \Phi(x, y) g(y) \right] ds(y),\ x \in \mathbb{R}^2 \backslash \bar{D}_2.$$

2. Select two lines $L_1 = \{(a_1, t),\ t \in \mathbb{R}\}$ and $L_2 = \{(t, a_2),\ t \in \mathbb{R}\}$, where $a_i \in \mathbb{R}$ are chosen so that the lines L_i are out of $D_2,\ i = 1, 2$.
3. Determine the points $z_i \in L_i : H(z_i) = \min\limits_{z \in L_i} H(z, f_2, g_2),\ i = 1, 2$.

4. Construct orthogonal lines to L_i passing through the points z_i, $i = 1, 2$.
5. The intersection point $P(d_1, d_2) \in D_1$ of the constructed orthogonal lines is considered as the initial approximation for the inclusion location.

4.2. Size estimation algorithm

This method relies on the assumption that the inclusion D_1 can be approximated by a circle B_{r_0} of unknown radius r_0 (more detailed in [3], [10]). To determine an appropriate value of r_0, we minimize a misfit function

$$T(r) = \left| \sum_{j=0}^{2n-1} (g_2(t_j) - g_r(t_j)) f_2(t_j) \right|, \tag{16}$$

that quantifies the difference between the observed boundary data and those computed from a corresponding auxiliary problem. The accuracy of the estimated inclusion size improves as this misfit decreases. Hence, the desired radius r_0 is identified as the value that satisfies the orthogonality condition

$$\int_{\Gamma_2} (g_2(y) - g_{r_0}(y)) f_2(y) ds(y) = 0,$$

which is necessary criteria for optimality. Here g_{r_0} represents the boundary data generated by the auxiliary problem with the inclusion approximated as a circle of radius r_0.

1. Consider the auxiliary Dirichlet problem

$$\Delta v = 0 \quad \text{in } \tilde{D},$$

$$v = 0 \quad \text{on } B_r, \quad v = f \quad \text{on } \Gamma_2,$$

where B_r is a circle centered at the point P, obtained by the line location search method and $\tilde{D} = D_2 \backslash \bar{B}_r$.

2. Compute the normal derivative $g_r = \frac{\partial v}{\partial \nu}$ on the boundary Γ_2.
3. Evaluate the function (16) for $r \in [R_0, R_1]$ and determine the radius r_0 such that

$$T(r_0) = \min_{r \in [R_0, R_1]} T(r).$$

The interval $[R_0, R_1]$ is selected to represent the feasible range of the size parameter, ensuring that the estimated size remains within the outer boundary.

5. Numerical experiments

In this section we present numerical experiment for Algorithm A, since the result obtained for Algorithm B for exact solution coincides completely. In case of noisy input data there is minor difference in comparison with another algorithm.

To demonstrate the effectiveness of the proposed method for solving the inverse problem, we use synthetic Cauchy data generated for known geometries. We consider an exterior boundary defined by

$$\Gamma_2 = \{x_2(t) = (2\cos t, 2\sin t),\ t \in [0, 2\pi]\}$$

and an interior boundary given by

$$\Gamma_1 = \{x_1(t) = (1 + 0.2\cos 3t)(\cos t, \sin t),\ t \in [0, 2\pi]\}\,.$$

The Cauchy data on Γ_2 is produced by solving the direct problem (1) – (3) with Dirichlet data $f_2 = 1$ and computing the Neumann data g_2 as the normal derivative on Γ_2. To simulate measurement errors, noisy data are modeled as

$$g_2^\delta = g_2 + \delta(2\eta - 1)||g_2||_{L_2(\Gamma_2)},$$

where δ is the noise level and $\eta \in (0, 1)$ is a uniformly distributed random variable.

Then we find the initial approximation for using iterative scheme. According to the line location search method, we consider two lines defined as $L_1 = \{(3, t),\ t \in \mathbb{R}\}$ and $L_2 = \{(t, -5.5),\ t \in \mathbb{R}\}$ for use in the line location search method. As a result, we obtain the intersection point of the lines orthogonal to L_1 and L_2, which is taken as the center of the initial approximation for the unknown boundary (see Fig. 1).

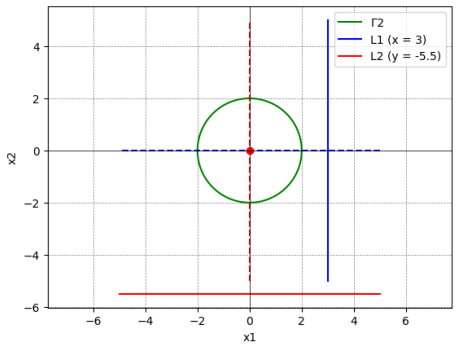

Fig. 1. Intial guess localization

For the size estimation algorithm we select an interval $[R_0, R_1]$ within the range from 0.1 to 1.9, ensuring that the search remains entirely within the outer boundary. Fig. 2 illustrates the dependency the parameter $r \in [R_0, R_1]$ on the corresponding values of the function $T(r)$.

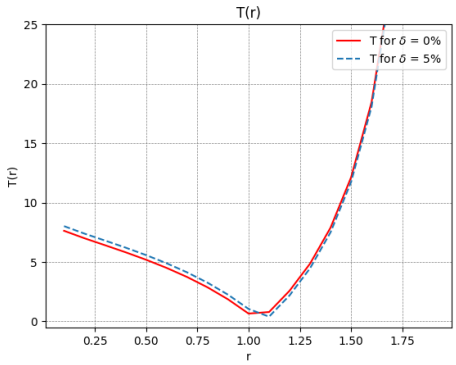

Fig. 2. Plot of the function T

As a result of applying both the location search and size estimation algorithms, the initial approximation is taken to be the unit circle centered at the origin for exact input data, and a circle of radius 1.1 centered at the origin for input data contaminated with 5% of noise.

Fig. 3 presents the reconstruction results for both exact and noisy data with $\delta = 5\%$, using discretization parameters $n = 16, m = 4, \alpha, \beta, \gamma = 1e{-}2, \zeta = 0.2, \xi = 0.7, \epsilon = 1e{-}3$.

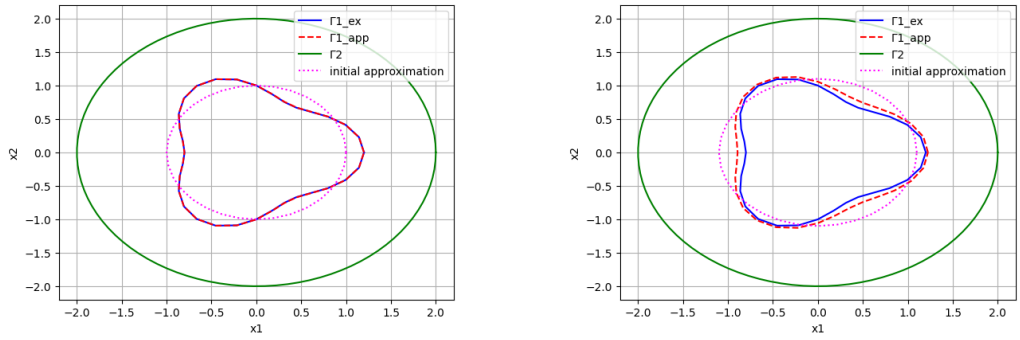

a Exact input data ***b*** Input data with 5% of noise

Fig. 3. The reconstructed interior boundary (exact Γ_1 – solid line, reconstructed Γ_1 – dashed line, initial guess of Γ_1 – dotted line)

As we can see from the Fig. 3 the reconstructed internal boundary coincides perfectly with the true boundary shape for exact input data. In contrast, when we have noisy data, a slight deviation is observed, however, it remains insignificant. It should be noted that selection of both relaxation and regularization parameters is essential, as they significantly influence the quality of the reconstruction under noisy conditions. Inappropriate values may lead to either oversmoothing or noise amplification.

6. Conclusion

In this paper we addresses the problem of reconstructing the inner boundary in a doubly-connected domain for the Laplace equation, using given Cauchy data and employing the integral equation method. The solution strategy is built around iterative algorithms, which involve solving the direct problem and applying a linearization of the integral equations. Particular emphasis was placed on selecting an appropriate initial guess to ensure convergence and preserve numerical stability. As part of the linearization process, the Fréchet derivative of the relevant integral equations was derived. Given the problem's inherent ill-posedness, a regularization technique was employed, allowing for stable solutions even in the presence of noisy input data. The resulting numerical experiments confirm the effectiveness of the proposed approach and highlight its potential for application to a variety of problems with specific physical significance.

References

1. Chapko R.S. On the non-linear integral equation approaches for the boundary reconstruction in double-connected planar domains / R.S. Chapko, O.M. Ivanyshyn Yaman, T.S. Kanafotskyi // Journal of Numerical and Applied Mathematics. – 2016. – Vol. 122. – P. 7–20.

2. Chapko R.S. On the non-linear integral equation method for the reconstruction of an inclusion in the elastic body / R.S. Chapko, O.M. Ivanyshyn Yaman, V.G. Vavrychuk // Journal of Numerical and Applied Mathematics. – 2019. – Vol. 130. – P. 7–17.
3. Chapko R. Location search technique and size estimation of the bounded inclusion for some inverse boundary value problems / R. Chapko, N. Vintonyak // Visnyk Khmelnytskogo universytetu. – 2007. – Vol. 93, № 2. – P. 186–191.
4. Cheng J. Uniqueness in an inverse boundary problem for Laplace's equation / J. Cheng, M. Yamamoto // Inverse Problems – 1996. – Vol. 12. – P. 213–219.
5. Ivanyshyn O. Nonlinear integral equations for solving inverse boundary value problems for inclusions and cracks / O. Ivanyshyn, R. Kress // J. Integral Equations Appl. – 2006. – Vol. 18. – P. 13–38.
6. Kim S. Location search technique for a grounded conductor / S. Kim, O. Kwon, J.K. Seo // SIAM J. Appl. Math. – 2002. – Vol. 62, № 4. – P. 1383–1393.
7. Kress R. Linear Integral Equations / R. Kress. – Springer, 2014.
8. Kress R. Numerical analysis / R. Kress. – Springer, 1998.
9. Kress R. Nonlinear integral equations and the iterative solution for an inverse boundary value problem / R. Kress, W. Rundell // Inverse Problems. – 2005. – Vol. 21. – P. 1207–1223.
10. Kwon O. Total size estimation and identification of multiple anomalies in the inverse conductivity problem / O. Kwon, J.K. Seo // Inverse Problems. – 2001. – Vol. 17. – P. 59–75.

Article: received 20.08.2025
revised 17.09.2025
printing adoption 24.09.2025

МЕТОД НЕЛІНІЙНИХ ІНТЕГРАЛЬНИХ РІВНЯНЬ ДЛЯ ОБЕРНЕНОЇ ЗАДАЧІ РЕКОНСТРУКЦІЇ МЕЖІ

Р. Хапко, С. Сенів

Львівський національний університет імені Івана Франка,
вул. Університетська 1, Львів, 79000, Україна
e-mail: roman.chapko@lnu.edu.ua, sofiia.seniv.pmp@lnu.edu.ua

У цій роботі розглядається задача відновлення внутрішньої межі двозв'язної області на площині за заданими даними Коші гармонічної функції на зовнішній межі. Використовуючи подання через потенціал простого шару, проблему зведено до системи нелінійних граничних інтегральних рівнянь. Запропоновано та реалізовано два ітераційні методи Ньютона для чисельного розв'язання цієї системи. Обчислено похідні Фреше відповідних інтегральних операторів. Повна дискретизація здійснена за допомогою методу квадратур та методу колокації. Для вирішення некоректності отриманої лінійної системи застосовано регуляризацію Філліпса-Тіхонова. Для пошуку початкового наближення до внутрішньої межі використовується метод прямих та алгоритм оцінки розміру. Обидва методи ґрунтуються на знаходженні мінімуму функціоналів, які включають задані дані Коші. Наведені чисельні приклади підтверджують стабільність, точність та обчислювальну ефективність запропонованого підходу.

Ключові слова: обернена задача, нелінійна задача, реконструкція межі, двозв'язна область, потенціал простого шару, метод інтегральних рівнянь, метод квадратур, похідна Фреше, регуляризація Філліпса-Тіхонова.